SUPPLEMENTARY DATA

Mercury enrichments and the Frasnian-Famennian biotic crisis: A volcanic trigger proved?

Grzegorz Racki, Michał Rakociński, Leszek Marynowski. Paul B. Wignall

(DR 1) SCHEME OF THE FRASNIAN-FAMENNIAN GLOBAL CHANGE

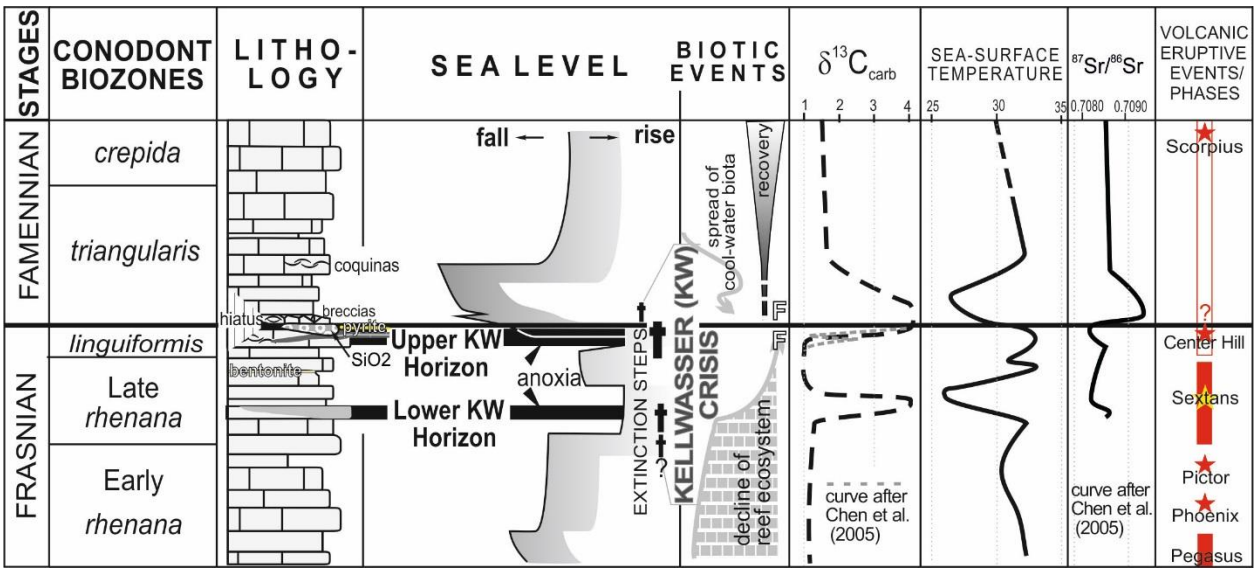

Diagram showing composite sedimentary and geochemical records across the Frasnian–Famennian transition, and major eustatic and biotic events (modified fig. 3 from Racki, 2005, and references therein; compare Joachimski and Buggisch, 2002, fig. 2; Gereke and Schindler, 2012, fig. 1 and 9; Ma et al., 2016, fig. 11); volcanic events after Winter (2015, fig. 2).

(DR 2) ANALYTICAL SECTIONS

The successions listed below were recently studied, in different extent, within the program of MAESTRO grant 2013/08/A/ST10/00717 (to Grzegorz Racki) from Polish National

Science Foundation. Archival samples only from German and Russian localities were re-analyzed recently for Hg abundances.

Enrichment Hg patterns are shown for samples revealing values distinctly greater than background (= threefold median value as a given threshold; cf. Riboulleau et al., 2018) in the succession. The recurrence of enrichment factors larger than 3 for Hg/TOC and Hg/Al_2O_3, along with less rigorously determined values for absolute Hg abundances, identifies the highlighted sample in tables below as truly enriched one (or likely/possibly enriched one, where not all requirements are fulfilled). On the other hand, the distinctive Hg impoverishment in at least one of these test indicators eliminates the sample from consideration as enriched.

The statistical calculations were carried out using PAST 1.94b (Hammer, 2009); significant correlations with a p-value less than 0.01 are given in bold type.

In the tables below, time intervals of the anoxic Kellwasser events are highlighted in light gray, whilst black shale facies is shown in dark gray.

1. Lahmida section, eastern Anti-Atlas, Morocco

Coordinates: 31°30'67.0'' N; 4°19'26.2'' W

The Lahmida section, located ca. 12 km to north-west from Erfoud in the eastern part of the Anti-Atlas, accumulated on the deep-water Rheris shelf basin, which stretched to north from Tafilalt Platform (Dopieralska, 2003, 2009). The investigated succession stratigraphically extends from the lower Frasnian - MN Zone 4 to the middle Famennian *rhomboidea* Zone (see Dopieralska, 2003). The succession consists mainly of monotonous shales with numerous marly interbeds and concretion horizons as well as dark gray limestones, which together with dark gray shales represent the Kellwasser facies of the Rheris Basin (Wendt and Belka, 1991; for more details about geology see Dopieralska, 2003).

We analyzed 43 samples, collected in 2014 and 2015 for the MAESTRO grant with the help of Zdzisław Bełka.

Hg, TOC, Al_2O_3, Mo contents, and Hg/TOC and Hg/Al_2O_3 ratios from F-F succession at Lahmida.

Stage	Sample	Hg	TOC	Al_2O_3	Mo	Hg/TOC	Hg/ Al_2O_3	Height (cm)
	Method	AAS	Eltra CS-	ICP-ES	ICP-MS			
		ppb	%	%	ppm			
	Max. detection limit (MDL)	0.2	0.01	0.01	0.1			
	LA 44	54.5	0.61	4.83	1.0	89.3	11.3	3575
	LA 43/44	31.2	0.68	5.23	1.3	45.9	6.0	3555
	LA 42	250.0	0.83	5.85	4.4	301.2	42.7	3455
	LA 41/42	276.6	1.14	21.90	5.8	242.6	12.6	3405
	LA 40T	44.8	0.59	3.37	0.3	75.9	13.3	3159
	LA 38	99.8	0.42	2.93	0.9	237.6	34.1	2918
	LA 35/36B	283.2	0.83	20.60	0.7	341.2	13.7	2687
	LA 34	260.0	0.75	5.50	0.3	346.7	47.3	2350
	LA 32/33	207.0	0.46	20.72	1.4	450.0	10.0	2093
	LA 32M	153.2	0.38	2.61	1.5	403.2	58.7	2040
	LA 30	333.8	0.86	3.58	1.6	388.1	93.2	1781
	LH 29	137.5	0.11	1.73	4.6	1250.0	79.5	1670
	LH 28	114.0	0.40	5.41	1.1	285.0	21.1	1635
	LH 27A2	569.1	0.93	21.04	1.9	611.9	27.0	1614
	LA 27/28	338.4	1.05	20.70	2.7	322.3	16.3	1569
	LH 27	126.4	0.77	4.97	4.9	164.2	25.4	1538
	LA 26/27	481.2	0.86	21.02	2.3	559.5	22.9	1516
	LH 26	57.3	0.55	2.43	3.3	104.2	23.6	1497
	LA 25/26	232.5	0.54	18.85	2.5	430.6	12.3	1464
	LH 25T	180.1	0.79	3.10	0.9	228.0	58.1	1437
FAMENNIAN	LH 25B	189.3	0.37	2.57	2.3	511.6	73.7	1423
FRASNIAN	LA 24/25S	36.9	0.35	3.17	1.6	105.4	11.6	1413
	LA 24/25N **CH**	1136.4	0.16	2.33	0.9	7102.5	487.7	1403
	LH 24T	113.2	0.65	2.79	2.0	174.2	40.6	1395
	LH 24B **?**	153.7	0.10	0.96	0.9	1537.0	160.1	1383
Upper KW	LH 23T	219.0	0.67	1.99	4.4	326.9	110.1	1374
	LH 23B	90.0	0.13	4.24	9.9	692.3	21.2	1366
	LH 22 **?**	464.2	0.41	2.08	15.0	1132.2	223.2	1343
	LH 21	90.3	0.11	3.21	3.1	820.9	28.1	1215
	LH 20	45.7	0.01	2.41	1.2	4570.0	19.0	1178
	LH 19	123.0	0.76	2.49	1.3	161.8	49.4	1138
	LH 18	187.7	0.20	0.93	5.0	938.5	201.8	1089
Lower KW	LA 17/18T**?Sx**	183.2	0.03	1.04	1.6	6106.7	176.2	1045
	LA 17/18B	147.8	0.37	1.61	1.5	399.5		1020
	LA 17M	99.9	0.24	2.75	2.0	416.3	36.3	989
	LA 14 **PPP**	1144.9	0.56	3.49	4.6	2044.5	328.1	875
	LA 13T	233.1	0.71	1.05	1.7	328.3	222.0	836
	LA 12	68.8	0.41	3.78	0.5	167.8	18.2	735
	LA 10	6.8	0.32	2.09	0.5	21.3	3.3	602
	LA 8	9.9	0.28	1.71	<0.1*	35.4	5.8	418
	LA 6	25.9	0.33	2.29	0.2	78.5	11.3	268
	LA 5	312.3	0.48	1.55	3.1	650.6	201.5	198
	LA 4A	36.9	1.21	1.84	1.6	30.5	20.1	101
Median value		**153.2**	0.48	2.93	1.6	341.2	28.1	
Spearman's rs correlation coefficient coefficient		Hg	0.37	0.24	**0.40**			

*Mo assumed as 0.09 ppm for purpose of the correlation calculation

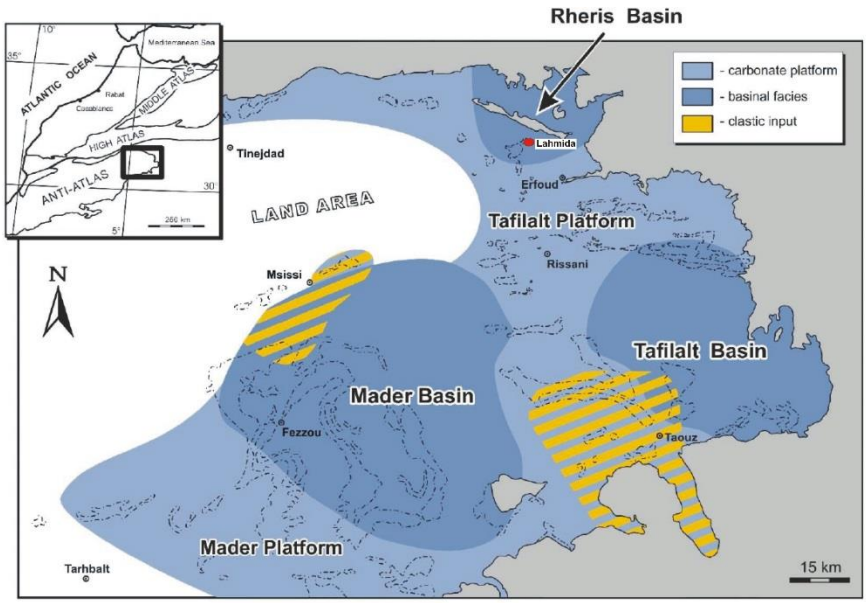

S 1. Geographic and palaeogeographic location of the Lahmida section (Bełka and Wendt, 1992; Dopieralska, 2003).

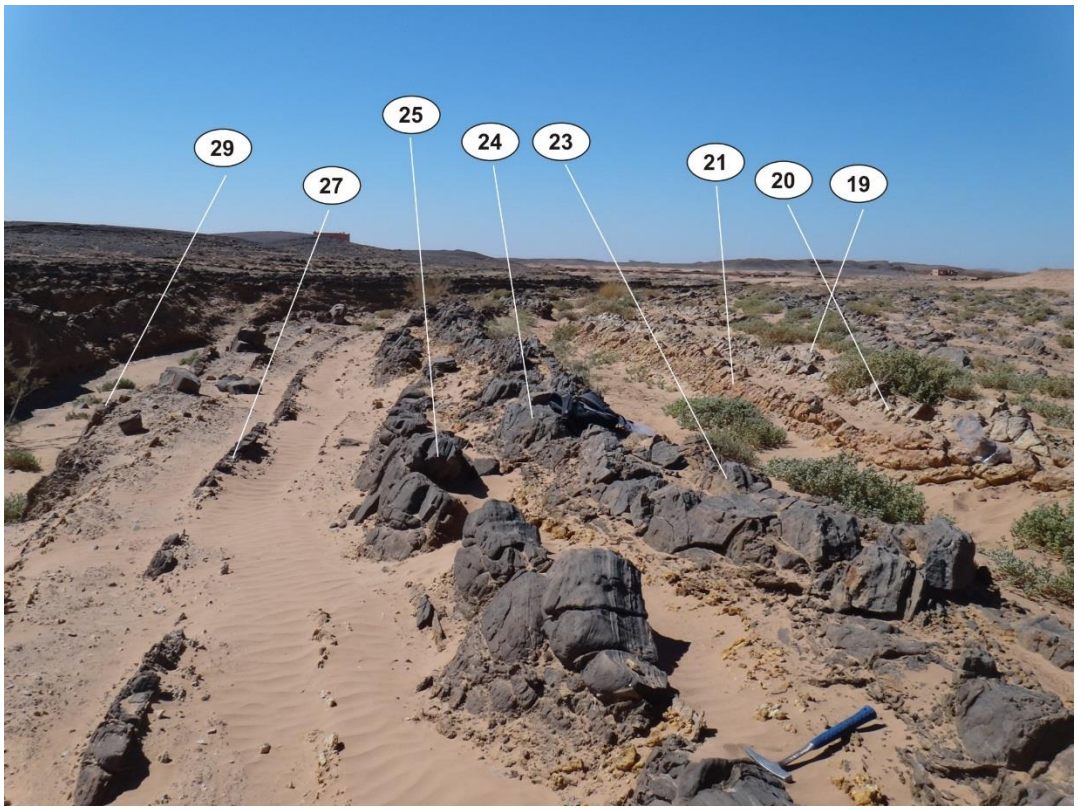

S 2. The Frasnian-Famennian boundary beds at Lahmida section (March 2014), with the stage boundary located between beds 24 and 25. Photo courtesy Z. Bełka.

2. Kahlleite, Thuringia, Germany

Coordinates: 50°37'32.5''; N; 11°50'32.2'' E

The Frasnian-Famennian transition at inactive (since 2013) Kahlleite quarry, 1 km to south-west from Rüdersdorf near Gera, Thuringia, was studied by Gereke (2004, 2007). The mainly limestone strata of the north-west flank of Berga Anticline deposited on a deep submarine rise (Gereke and Schindler, 2012). The Upper KW interval is implicitly interpreted as encompassing the upper part of the *linguiformis* conodont zone in this site, and not only very thin KW black shale in its top.

This locality was sampled in 2012 by L.M. and M.R., guided by Manfred Gereke, and 17 samples were recently re-studied for Hg.

Hg, Al_2O_3, Mo contents, and Hg/TOC and Hg/Al_2O_3 ratios from F-F succession at Kahlleite.

Stage	Sample	Hg (ppb)	TOC	Al_2O_3	Mo	Hg/TOC	Hg/ Al_2O_3	Height (cm)
	Method	AAS	Eltra CS-500	ICP-ES	ICP-MS			
		ppb	%	%	ppm			
	MDL	0,2		0.01	0.1			
	K 8	16.2	0.79	5.28	0.4	20.5	3.1	408.5
	K 7	6.9	0.68	5.29	0.2	10.1	1.3	353.5
	K 6	11.0	0.19	19.45	0.1	57.9	0.6	308.5
	K 5	5.2	0.67	4.17	0.1	7.8	1.2	263.5
	K 4	8.5	0.65	2.97	0.1	13.1	2.9	243.5
	K 3	9.3	0.72	1.75	0.1	12.9	5.3	231.5
	K 2	18.9	0.59	4.89	0.5	32.0	3.9	223.5
FAMENNIAN	K 1	22.5	0.71	3.81	1.4	31.7	5.9	208.5
FRASNIAN	K 0 CH	2517.3	7.04	17.21	40.8	357.6	146.3	203
Upper KW	K 01 ?CH	93.0	0.64	5.98	2.0	145.3	15.6	201
	K 02	22.7	0.64	5.82	0.2	35.5	3.9	200
	K 03	23.6	0.31	17.09	0.5	76.1	1.4	185
Inter KW	K 05	10.6	0.70	3.29	0.1	15.1	3.2	145
	K 06	36.4	0.59	5.42	0.1	61.7	6.7	95
	K 07 ?Sx	63.3	0.43	15.49	0.1	147.2	4.1	55
	K 08	42.1	0.82	1.52	0.1	51.3	27.7	23
Median value		**20.7**	0.66	5.29	0.15	32.0	3.9	
Spearman's rs correlation coefficient		Hg	0.05	0.44	0.44			

?Volcaniclastics

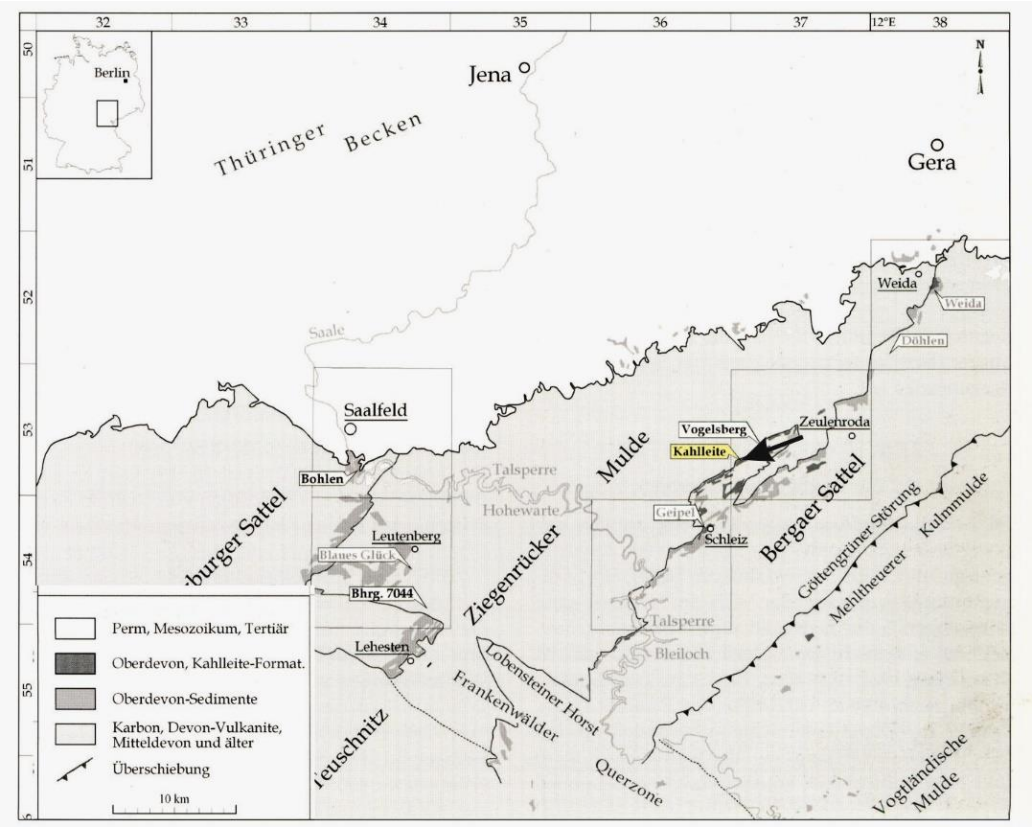

S 3. Location of Kahlleite section (arrowed) in central Germany (from Gereke, 2007).

S 4. General view of the quarry wall exposing the upper Frasnian and the F-F boundary interval (left), and close-up of the F-F boundary beds at Kahlleite (September 2012; right).

3. Syv'yu, Subpolar Urals, north-eastern European Russia

Coordinates: 65°45'58.2" N; 59°30'30.8" E

The deep-slope succession of the Timan−Pechora Basin, West−Urals structural zone, was studied by Yudina et al. (2002). The Syv'yu River section is located in the vicinity of the town of Inta (Subpolar Urals) near Vorkuta (Komi Republic), about 38 km up-stream from its junction with the Kozhym River. The Upper Devonian deposits, exposed along the right bank of Syv'yu River in several outcrops, represent an almost continuous sequence of the clayey-siliceous-carbonate (Domanic−type) deposits through the Frasnian and lower Famennian, and comprise thinly bedded, westerly dipping strata, without tectonic complications.

For present paper, 62 archival samples, from a densely sampled 7.8 m interval, yielded in 1999 by Alexandra Yudina, were re-measured.

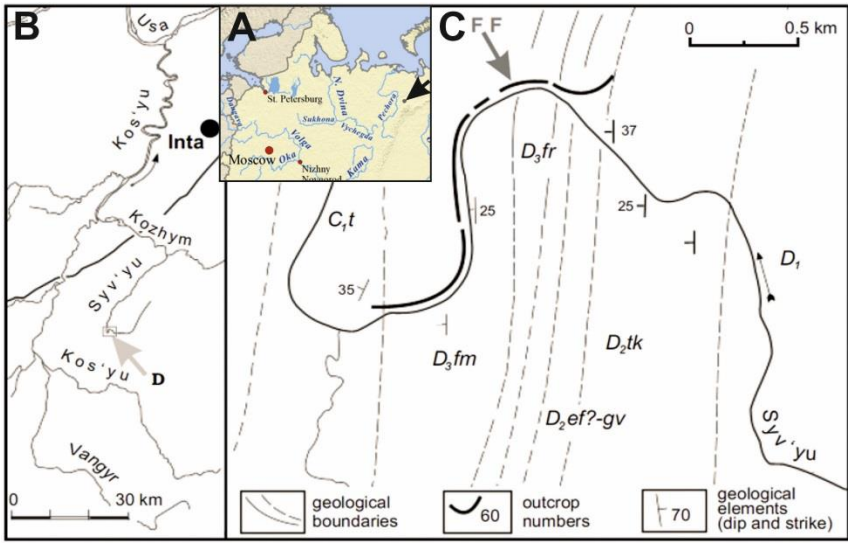

S 5. Location of Syv'yu locality in northern European Russia (A), Kozhym River basin (B), and locality map of studied outcrops along the Syv'yu River section, western slopes of the Subpolar Urals (C); C1t, Tournaisian; D1, Lower Devonian; D2tk, ?Middle Devonian, Takata Suite; D2ef−gv, Eifelian–Givetian; D3fr, Frasnian; D3fm, Famennian (from Yudina et al., 2002, fig. 1).

Hg, Al_2O_3, Mo contents, and Hg/TOC and Hg/Al_2O_3 ratios from F-F succession of Syv'yu River.

Stage	Sample	**Hg**	**TOC**	**Al_2O_3**	**Mo**	**Hg/ TOC**	**Hg/ Al_2O_3**	**Height (cm)**
	Method	AAS	Eltra CS-500	ICP-ES	INAA			
		ppb	%	%	ppm			
	MDL	0.2	0.01	0.01	2 or 5			
	SYV 96 - S10	21.8	2.24	no data	no data	9.8	x	775
	SYV 96 - S12	23.2	1.64	no data	no data	14.1	x	748,5
	SYV 96 - S 9	21.8	2.19	no data	no data	10.1	x	739,5

	SYV 96 - S7	16.4	1.46	no data	no data	11.0	x	714,5
	SYV 96 - S4	15.3	2.79	no data	no data	5.4	x	651,5
	SYV 96 - 134A	12.9	1.89	0.21	<5	6.9	61.5	613,5
	SYV 96 - 132	23.5	3.09	no data	no data	7.5	x	599
	CB 99355	24.2	1.39	0.33	<5	17.2	73.4	591
	CB 99354	36.8	1.40	0.34	<5	26.5	108.2	585,5
	CB 99353	26.6	1.64	0.43	<5	27.4	104.5	582,5
	CB 99352	43.0	2.04	0.48	<5	21.1	89.6	581,5
	CB 99351	44.9	2.40	0.63	<5	19.6	74.9	578
	CB 99350	47.2	2.0	0.87	<5	23.57	54.3	575,5
	CB 99349	33.8	2.00	0.39	<5	17.0	86.5	573,5
Famennian	SYV 96 - 138/1	26.9	2.13	0.27	<5	12.7	99.8	571,5
Frasnian	CB 99348	50.5	2.66	0.24	<5	19.2	210.4	570,5
	CB 99347* ” **CH**	120.8	1.33	0.19	<2	90.9	636.8	568,5
	CB 99346	109.8	2.11	0.30	<5	52.2	366.0	566,5
	CB 99345” ?**CH**	109.6	1.65	0.07	<2	66.5	1571.4	564,5
	CB 99344	89.9	2.47	0.15	<5	36.5	599.3	561,5
	CB 99342	65.4	1.97	0.22	<5	33.1	297.4	556,5
	CB 99341	39.7	3.00	0.45	<5	13.3	88.2	555,5
	CB 99340	153.6	3.05	0.68	<5	50.5	225.9	554,5
	CB 99339 ?	162.2	2.41	0.56	<5	67.3	289.6	553,5
	CB 99338	111.2	2.65	0.55	6	42.0	202.1	552,5
	CB 99337 ?	237.0	2.10	1.09	<5	112.9	217.4	550,5
	CB 99336 ?	260.5	2.32	0.44	<5	112.2	591.9	549,5
	CB 99335	41.6	2.17	0.54	<5	19.3	77.1	546,5
	CB 99334	93.5	4.18	1.26	<5	22.2	74.2	543,5
Upper KW	CB 99333	132.6	3.71	1.09	<5	35.9	121.7	542
	CB 99332	42.8	3.48	1.14	<5	12.3	37.5	539,5
	CB 99331	42.2	4.05	1.13	<5	10.4	37.3	537
	CB 99330	24.5	3.35	0.54	<5	7.2	45.3	535
	CB 99329	23.8	3.00	0.38	<5	8.0	62.7	531,5
	CB 99328	36.7	3.13	0.36	<5	11.8	101.9	526,5
	CB 99327 ?	233.9	2.81	0.98	25	83.3	238.6	523,5
	CB 99326	41.3	2.58	1.15	<5	15.9	35.9	521,5
	CB 99325	191.6	5.54	9.66	17	34.7	19.8	513
	CB 99323	96.4	2.37	6.24	8	40.6	15.4	502
	CB 99322	59.5	2.73	6.75	<5	22.0	8.8	495,5
	CB 99321	49.5	3.12	5.71	<5	15.7	8.7	492
	CB 99320	107.5	2.09	10.99	<5	51.1	9.8	481,5
	CB 99318 **?Sx**	212.6	2.84	1.95	<5	74.9	109.0	458,5
	CB 99317	61.5	1.36	2.09	<5	45.6	29.4	451,5
	CB 99316 **?Sx**	221.5	1.84	10.92	<5	120.0	20.3	443
	CB 99314	109.2	2.08	11.23	<5	52.4	9.7	427,5
	CB 99313	36.7	2.24	2.18	<5	16.6	16.9	419
	CB 99312	59.5	1.16	13.75	<5	51.0	4.3	415,5
	CB 99310	25.1	1.81	1.49	<5	13.8	16.9	399
	CB 99309	94.1	2.11	7.66	<5	44.6	12.3	391
	CB 99305	25.4	1.55	2.02	<5	16.1	12.6	351,5
Inter KW	CB 99301	32.9	1.38	2.57	<5	23.9	12.8	305,5
	CB 99300	46.1	0.62	15.79	<5	74.2	2.9	297,5
	CB 99229	18.5	1.75	1.64	<5	10.3	11.3	295
	CB 99228	36.4	1.90	1.80	<5	18.9	20.2	288
	CB 99227	51.7	2.28	7.04	<5	22.8	7.3	282,5
	CB 99226	16.4	1.83	1.11	<5	8.8	14.8	275
	SYV 96 - 100	37.3	1.84	1.18	<5	20.1	31.6	220
	SYV 96 - 91	17.1	2.92	no data	no data	5.8	x	67
	CB 99222	36.4	0.83	0.49	<5	43.2	74.3	0

	CB 9921	37.0	1.27	no data	no data	29.1	x	Omitted in Fig.
	SYV 96 – 64	18.7	1.62	no data	no data	11.7	x	
Median value		**42.5**	2.17	1.14	x	21.5	62.7	
Spearman's rs correlation		Hg	0.23	017	x			

*Samples analyzed in more refined variant

Zr enrichment (up to eightfold) and probable volcaniclastic admixture (Na−feldspars, micas, illite–smectite mixed layer clays, amorphous particles of ?glass shards; Yudina et al., 2002, fig. 7)

(DR 3) ANALYTHICAL METHODS

Mercury determination

Bulk samples from Lahmida and Kahlleite (and other nine) sections were first analyzed geochemically for trace elements at the Bureau Veritas AcmeLabs, Vancouver, Canada. Mercury concentrations were preliminarily determined using the conventional ICP-MS method (detection level of 10 ppb). Numerous high Hg values were established in the measured samples from the KW interval (see also Racki et al., 2018 - submitted). Only single Russian samples were originally analyzed for Hg contents by INAA at the Activation Laboratories, Ontario, Canada, by Racka in Yudina et al. (2002); however, they yield values below the method detection level (1000 ppb; see geochemical data repository at https://www.researchgate.net/publication/323430010_Geochemical_database_-_The_Frasnian-Famennian_events_in_a_deep-shelf_succession_Subpolar_Urals_biotic_depositional_and_geochemical_records).

Subsequently, Hg determination of 122 samples from the three sections was refined using atomic absorption spectrometry (AAS) Milestone DMA-80 Direct Mercury Analyzer (http://www.milestonesrl.com/landing-page/dma-80/) in the Faculty of Earth Sciences, University of Silesia (Poland). This commonly used analyzer assess samples by thermal decomposition, Hg amalgamation and atomic absorption detection, and has a detection limit of 0.2 ppb. The DMA analytical curves were prepared with dilution of a 1 mg L-1 standard solution (Merck Darmstadt, Germany). Measurement of each sample was duplicate and analyses were repeated when the coefficient of variability of samples exceeds 5%. The instrument was calibrated using certified reference material INCT-OBTL-5 (tobacco leaves) prior to the measurement, with Hg content = 20.9 ppm. The measured error did not exceed 2%. In another Hg study, with use of the same

analyzer, accuracy and precision of the determinations was estimated as ca. 8 and 6.5%, respectively (Sabatino et al., 2018).

Total organic carbon (TOC)

Total carbon (TC) contents were determined using an Eltra CS-500 IR-analyzer with a TIC (total inorganic carbon) module. TC was determined using an infrared cell detector. TIC content was determined by infrared detector as carbon dioxide derived from carbonates reacted with 15% warm hydrochloric acid. TOC was calculated as the difference between TC and TIC. Instrument calibration used Eltra standards. Analysis were performed in Faculty of Earth Sciences, University of Silesia (Poland).

Aluminum and molybdenum determinations

Al and Mo concentrations (DR 2) were analyzed at Bureau Veritas AcmeLabs, Vancouver, Canada, with the exception of samples from Russia, which were analyzed at Activation Laboratories, Ontario, Canada (Yudina et al., 2002). Al content was determined using ICP-ES method and precision and accuracy of the results were better than 0.01 %. Mo concentration was determined by ICP-MS method (detection level = 0.01 ppm; Lahmida, Kahlleite) or in two analytical variants by INAA (detection level = 2 and 5 ppm; Syv'yu).

(DR 4) THE STRONGEST HG AND HG/TOC SIGNALS OF THE "BIG FIVE" MASS EXTINCTIONS

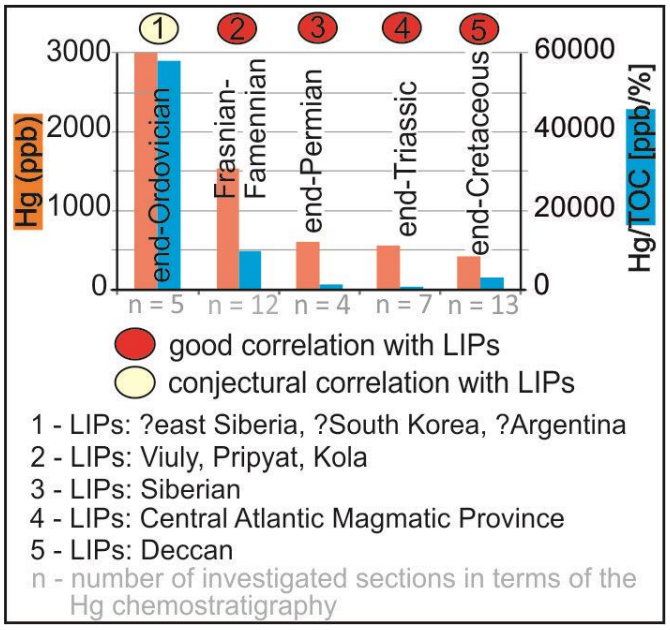

K-P: Nascimento Silva et al. (2011, 2013), Sial et al. (2013, 2014, 2016), Font et al. (2016)

J-T: Thibodeau et al. (2016), Percival et al. (2017)

P-T: Sanei et al. (2012), Grasby et al. (2013, 2015, 2017)

O-S: Jones et al. (2017), Gong et al. (2017)

REFERENCES CITED

Dopieralska, J., 2003, Neodymium isotopic composition of conodonts as a palaeoceanographic proxy in the Variscan oceanic system [Ph.D. Thesis]: Justus-Liebig-University, Giessen, 111 p.

Dopieralska, J., 2009, Reconstructing seawater circulation on the Moroccan shelf of Gondwana during the Late Devonian: Evidence from Nd isotope composition of conodonts: Geochemistry, Geophysics, Geosystems, v. 10 (3). p. 1-10, doi: 10.1029/2008GC002247.

Font, E., Adatte, T., Sial, A.N., de Lacerda, L.D., Keller, G., and Punekar, J., 2016, Mercury anomaly, Deccan volcanism, and the end-Cretaceous mass extinction: Geology, v. 44, p. 171–174, doi: 10 .1130 /G37451 .1.

Gereke, M., 2004, Das Profil Kahlleite Ost - die stratigraphische Entwicklung einer Tiefschwelle im Oberdevon des Bergaer Sattels (Thüringen): Geologica et Palaeontologica, v. 38, p. 1–31.

Gereke, M., 2007, Die oberdevonische Kellwasser-Krise in der Beckenfazies von Rhenoherzynikum und Saxothuringikum (spätes Frasnium/frühestes Famennium, Deutschland): Kölner Forum für Geologie und Paläontologie, v. 17, p. 1–228.

Gereke, M., and Schindler, E., 2012, "Time-Specific Facies" and biological crises — The Kellwasser Event interval near the Frasnian/Famennian boundary (Late Devonian): Palaeogeography, Palaeoclimatology, Palaeoecology, v. 367–368, p. 19–29, doi: 10.1016/j.palaeo.2011.11.024.

Gong, Q., Wang, X., Zhao, L., Grasby, S.E., Chen, Z-Q., Zhang, L., Li, Y., Cao, L., and Li, Z., 2017, Mercury spikes suggest volcanic driver of the Ordovician-Silurian mass extinction: Scientific Reports, v. 7, p. 1-7, doi: 10.1038/S41598-017-05524-5.

Grasby, S.E., Sanei, H., Beauchamp, B., and Chen, Z., 2013, Mercury deposition through the Permo- Triassic biotic crisis: Chemical Geology, v. 351, p. 209–216, doi: 10 .1016 /j .chemgeo .2013 .05 .022.

Grasby, S.E., Beauchamp, B., Bond, D.P.G., Wignall, P.B., and Sanei, H., 2015, Mercury anomalies associated with three extinction events (Capitanian crisis, latest Permian extinction and the Smithian/Spathian extinction) in NW Pangea: Geological Magazine, v. 153, p. 285–297, doi: 10 .1017 /S0016756815000436.

Grasby, S.E., Shen, W., Yin, R., Gleason, J.D., Blum, J.D., Lepak, R.F., Hurley, J.P., Beauchamp, B., 2017, Isotopic signatures of mercury contamination in latest Permian oceans: Geology, v. 45, p. 55-58, doi:10.1130/G38487.1.

Hammer, Ø., 1999-2009, PAST PAleontological Statistics Version 1.94b. Reference manual: Natural History Museum, University of Oslo, 175 p.

Joachimski, M.M., and Buggisch, W., 2002, Conodont apatite $\delta^{18}O$ signatures indicate climatic cooling as a trigger of the Late Devonian mass extinction: Geology, v. 30, p. 711–714, https://doi.org/10.1130/0091-7613(2002)030<0711:CAOSIC>2.0.CO;2.

Jones, D.S., Martini, A.M., Fike, D.A., and Kaiho, K., 2017, A volcanic trigger for the Late Ordovician mass extinction? Mercury data from south China and Laurentia: Geology, v. 45, p. 631-634, doi:10.1130/G38940.1.

Ma, X., Gong, Y., Chen, D., Racki, G., Chen, X., and Liao, W., 2016, The Late Devonian Frasnian-Famennian event in South China—Patterns and causes of extinctions, sea level changes, and isotope variations: Palaeogeography, Palaeoclimatology, Palaeoecology, v. 448, p. 224–244, https://doi.org/10.016/j.palaeo.2015.10.047.

Nascimento-Silva, M.V., Sial, A.N., Ferreira, V.P., Neumann, V.H., Barbosa, J.A., Pimentel, M.M., and de Lacerda, L.D., 2011, Cretaceous-Paleogene transition at the Paraíba Basin, Northeastern, Brazil: Carbon-isotope and mercury subsurface stratigraphies: Journal of South American Earth Sciences, v. 32, p. 379–392, doi: 10.1016/j.jsames.2011.02.014.

Nascimento-Silva, M.V., Sial, A.N., Barbosa, J.A., Ferreira, V.P., Neumann, V.H., and de Lacerda, L.D., 2013, Carbon isotopes, rare-earth elements and mercury geochemistry across the K -T transition of the Paraíba Basin, northeastern Brazil, *in* Bojar, A.V., Melinte-Dobrinescu, M.C., and Smit, J., eds., Isotopic Studies in Cretaceous Research: Geological Society (London) Special Publications 382, p. 85-104, doi: 10.1144/SP382.2.

Percival, L.M.E., Ruhla, M., Hesselbo, S.P., Jenkyns, H.C., Mather, T.A., and Whiteside J.H., 2017, Mercury evidence for pulsed volcanism during the end-Triassic mass extinction: Proceedings of the National

Academy of Sciences of the United States of America, v. 114, p. 7929–7934, doi: 10.1073/pnas.1705378114.

Racki, G., 2005, Toward understanding Late Devonian global events: Few answers, many questions, *in* Over. D.J., Morrow, J.R., and Wignall, P.B., eds., Understanding Late Devonian and Permian–Triassic Biotic and Climatic Events: Amsterdam, Elsevier, Towards an Integrated Approach, Developments in Palaeontology and Stratigraphy 20, p. 5–36.

Racki, G., Marynowski, L., and Rakociński, M., 2018 (submitted). Anomalous Upper Devonian mercury enrichments: Inductively Coupled Plasma - Mass Spectrometry (ICP-MS) analytical data are reliable. Geological Quarterly.

Riboulleau, A., Spina, A., Vecoli, M., Riquier, L., Quijada, M., Tribovillard, N., and Averbuch, O., 2018, Organic matter deposition in the Ghadames Basin (Libya) during the Late Devonian: A multidisciplinary approach: Palaeogeography, Palaeoclimatology, Palaeoecology, v. 497, p. 37–51, doi: 10.1016/j.palaeo.2018.02.004.

Sabatino, N., Ferraro, S., Coccioni, R., Bonsignore M., Del Core, M., Tancredi, V., Sprovieri, M., 2018, Mercury anomalies in upper Aptian-lower Albian sediments from the Tethys realm: Palaeogeography, Palaeoclimatology, Palaeoecology, v. 495, p. 163–170, doi: 10.1016/j.palaeo.2018.01.008 .

Sanei, H., Grasby, S.E., and Beauchamp, B., 2012, Latest Permian mercury anomalies: Geology, v. 40, p. 63–66, doi:10.1130/G32596.1

Sial, A.N., Lacerda, L.D., Ferreira, V.P., Frei, R., Marquillas, R.A., Barbosa, J.A., Gaucher, C., Windmöller, C.C., and Pereira, N.S., 2013, Mercury as a proxy for volcanic activity during extreme environmental turnover: the Cretaceous–Paleogene transition: Palaeogeography, Palaeoclimatology, Palaeoecology, v. 387, p. 153–164, doi: 10.1016/j.palaeo.2013.07.019.

Sial, A.N., Chen, J.-B., Lacerda, L.D., Peralta, S., Gaucher, C., Frei, R., Cirilli, S., Ferreira, V.P., Marquillas, R.A., Barbosa, J.A., Pereira, N.S., and Belmino, I.K.C., 2014, High-resolution Hg chemostratigraphy: A contribution to the distinction of chemical fingerprints of the Deccan volcanism and Cretaceous–Paleogene boundary impact event: Palaeogeography, Palaeoclimatology, Palaeoecology, v. 414, p. 98–115, doi: 10.1016/j.palaeo.2014.08.013.

Sial, A.N., Chen, J., Lacerda, L.D., Frei, R., Tewari, V.C., Pandit, M.K., Gaucher, C., Ferreira, V.P., Cirilli, S., Peralta, S., Korte, C., Barbosa, J.A., and Pereira, N.S., 2016, Mercury enrichment and Hg isotopes in Cretaceous–Paleogene boundary successions: Links to volcanism and palaeoenvironmental impacts: Cretaceous Research, v. 66, p. 60–81, doi: 10.1016/j.cretres.2016.05.006.

Thibodeau, A.M., Ritterbush, K., Yager, J.A., West, A.J., Ibarra, Y., Bottjer, D.J., Berelson, W.M., Bergquist, B.A., and Corsetti, F.A., 2016, Mercury anomalies and the timing of biotic recovery following the end-Triassic mass extinction: Nature Communications, v. 7, p. 1-8, doi: 10 .1038 /ncomms11147.

Wendt, J., and Belka, Z., 1991, Age and depositional environment of Upper Devonian (Early Frasnian to Early Famennian) black shales and limestones (Kellwasser Facies) in the Eastern Anti-Atlas. Morocco: Facies, v. 25, p. 51-90, doi: 10.1007/BF02536755.

Winter, J., 2015, Vulkanismus und Kellwasser-Krise–Zirkon-Tephrostratigrafie, Identifizierung und Herkunft distaler Fallout-Aschenlagen (Oberdevon, Synklinorium von Dinant, Rheinisches Schiefergebirge, Harz):

Zeitschrift der Deutschen Gesellschaft für Geowissenschaften, v. 166, p. 227–251, https://doi.org/10.1127/1860-1804/2015/0092.

Yudina, A.B, Racki, G., Savage, N.S., Racka, M., and Małkowski, K., 2002, The Frasnian-Famennian events in a deep-shelf succession, Subpolar Urals: Biotic, depositional and geochemical records: Acta Palaeontologica Polonica, v. 47, p. 355-372.